academicJournals

Vol. 8(10), pp. 395-405, 16 March, 2013
DOI: 10.5897/IJPS12.524
ISSN 1992-1950 © 2013 Academic Journals
http://www.academicjournals.org/IJPS

International Journal of Physical Sciences

Full Length Research Paper

A modified surface wave particle motion discrimination process

Yusuf Arif Kutlu[1]* and Nilgün Sayıl[2]

[1]Department of Geophysics, Faculty of Engineering and Architecture, Nevsehir University, 50300, Nevsehir-Turkey.
[2]Department of Geophysics, Faculty of Engineering, Karadeniz Technical University, 61080, Trabzon-Turkey.

Accepted 11 March, 2013

The difference between polarization properties of surface waves and noise provides us with a simple way of discriminating the fundamental mode surface waves on three-component seismograms. In this process, vertical, radial and transverse component amplitudes at each frequency are weighted according to a theoretical three-dimensional particle motion pattern for a selected window length (WL) and moving interval (MI). For the epicentral distances closer than about 2200 km, the weighted functions of a formerly proposed approach are not compatible with the angular distributions of polarization properties of surface waves. It means that the former weighted functions are not perfectly able to weight surface waves amplitudes of some epicentral distances. In order to solve this problem, a modification in this study is implemented by analyzing compatibility of the weighted functions with the angular distribution of polarization properties of synthetic surface waves. The former and new processes are tested on three component synthetic seismograms and on some digital broadband records. As a result, the new filtering process (NFP) is shown to be more flexible and stable. It can be used to discriminate the fundamental mode Love and Rayleigh waves on three-component seismograms at all ranges of epicentral distances.

Key words: Former filtering process (FFP), surface wave particle motion discrimination process, new filtering process (NFP), modified surface wave particle motion discrimination process.

INTRODUCTION

Since 1960s, polarization analysis techniques for various types of data sets have been implemented to describe the signal content of time series in geophysics (Flinn, 1965; Samson, 1977; Samson and Olson, 1980; Holcomb, 1980; Kanasewich, 1981; Vidale, 1986; Plesinger et al., 1986; Jurkevics, 1988; Shieh and Herrmann, 1990; Perelberg and Hornbostel, 1994; Lilly and Park, 1995; Selby, 2001). And also several methods based on the polarization properties of different types of waves have been proposed to discriminate between signal and noise in time or frequency domain (Shimsoni and Smith, 1964; Simons, 1968; Montalbetti and Kanasewich, 1970; Blandford, 1977, 1982; Morozov and Smithson, 1996; Patane and Ferrari, 1997; Chael, 1997; Du et al., 2000; De Meersman et al., 2006; Pinnegar, 2006; Amoroso et al., 2012).

On long period seismograms, in order to isolate the fundamental mode Love and Rayleigh waves from the effects of microseismic noise, a surface wave particle motion discrimination process was designed by Simons (1968) using the differences of polarization properties between surface waves and microseismic noise. The weighted functions of this former filtering process (FFP) are not compatible with the angular distributions of polarization properties of the fundamental mode surface waves at epicentral distances closer than about 2200 km

*Corresponding author. E-mail: yakutlu@nevsehir.edu.tr. Tel: +90 384 2281162.Fax: +90 384 2281083.

due to time-frequency resolution loss depending mainly on the selection of window length (WL) and interval moving process. This case causes deformation of isolated fundamental mode surface waves on three-component seismograms. The aim of this study is to devise new weighted functions to solve this problem by adjusting the weighted functions according to the synthetic polarization parameters. In this respect, we made use of the compatibility between the angular distribution of polarization properties of the fundamental mode surface waves and the weighted functions of FFP. FFP and the newly proposed filtering process (NFP) are tested on three-component synthetic seismograms and also on digital broadband recordings with all ranges of epicentral distances.

SURFACE WAVE PARTICLE MOTION DISCRIMINATION PROCESS

This process is performed in the frequency domain because of the dispersive character of surface waves. Discrete Fourier transforms of vertical, radial and transverse component ground motions are calculated for a selected WL and then the interval is moved. Amplitude coefficients at each frequency are weighted according to three-dimensional theoretical particle motion pattern of Love and Rayleigh waves. The weights or adjustments do not apply to the original phase values. The weighted segments for each windowing are transformed back to the time domain, and the filtered signal is obtained after averaging over the overlapping amplitudes.

The components of the ground motion with length N.Δt (Δt sampling rate) are derived from Discrete Fourier coefficients according to the following equations:

$$A_i(\eta f) = \left[a_i^2(\eta f) + b_i^2(\eta f)\right]^{1/2}, \qquad \eta = 0, 1, 2, ..., N/2 \tag{1a}$$

$$\Phi_i(\eta f) = \arctan\left[\frac{b_i(\eta f)}{a_i(\eta f)}\right], \qquad \eta = 0, 1, 2, ..., N/2 \tag{1b}$$

Where i = Z, R, T define vertical, radial and transverse component ground motions, respectively. $A_Z(\eta f)$, $A_R(\eta f)$, $A_T(\eta f)$ are vertical, radial and transverse amplitudes at each frequency as shown in Figure 1.

In addition, $\beta(\eta f)$ is the apparent horizontal azimuth, $\psi(\eta f)$ is the angle between major eccentricity of the particle motion ellipse and vertical component, and $\alpha(\eta f)$ is the phase difference between vertical and radial components in Figure 1, which are calculated from the following equations:

$$\beta(\eta f) = \arctan\left[\frac{A_T(\eta f)}{A_R(\eta f)}\right] \tag{2a}$$

$$\psi(\eta f) = \arctan\left[\frac{\sqrt{A_R^2(\eta f) + A_T^2(\eta f)}}{A_Z(\eta f)}\right] \tag{2b}$$

$$\alpha(\eta f) = \phi_R(\eta f) - \phi_Z(\eta f) \tag{2c}$$

The spectral amplitudes at each frequency can be weighted using the functions $\beta(\eta f)$, $\psi(\eta f)$ and $\alpha(\eta f)$ as follows (Simons, 1968):

$$A_Z'(\eta f) = A_Z(\eta f).\cos^M\left[\beta(\eta f)\right].\cos^K\left[\psi(\eta f) - \theta\right].\sin^N\left[\alpha(\eta f)\right] \tag{3a}$$

$$A_R'(\eta f) = A_R(\eta f).\cos^M\left[\beta(\eta f)\right].\cos^K\left[\psi(\eta f) - \theta\right].\sin^N\left[\alpha(\eta f)\right] \tag{3b}$$

$$A_T'(\eta f) = A_T(\eta f).\sin^M\left[\beta(\eta f)\right].\sin^K\left[\psi(\eta f)\right] \tag{3c}$$

Herein $A'_Z(\eta f)$, $A'_R(\eta f)$ and $A'_T(\eta f)$ are the weighted vertical, radial and transverse components of the ground motion, respectively. The functions $\beta(\eta f)$, $\psi(\eta f)$ and $\alpha(\eta f)$ vary in the range from 0 to 1. The exponents M, K and N are empirically obtained as 8, 8 and 4. The angle θ can be set to 0.21π (37.8°) corresponding to the theoretical horizontal/vertical displacement ratio for the fundamental mode Rayleigh waves in the Gutenberg Earth model.

The modification of FFP

Depending on WL and MI, the weighted functions of FFP may not be compatible with the angular distribution of polarization parameters calculated from synthetic seismograms at each frequency for particularly smaller epicentral distances. This case of FFP causes weak detection of surface waves on three-component seismograms. Our objective is to find new weighted functions to overcome this problem by adjusting the weighted functions to the polarization parameters (Equations 2a, b and c). In order to investigate the compatibility issue, the synthetic surface waves were computed using two sets of parameters given in Tables 1 and 2.

We subsequently calculated the synthetic polarization parameters at each frequency for the specified time sections (Sections 1, 2, and 3 represent pure Love particle motion, pure Rayleigh particle motion and mixed particle motion, respectively in Figure 2) and obtained respective angular distributions in Figure 3. Also, to derive the synthetic polarization parameters of full length Love wave particle motion, we combined Section 1 with the right sides of Section 3 around 45° for β and around 60° for ψ, respectively in Figure 3. In a similar way, for full length Rayleigh wave particle motion, we combined Section 2 with the left sides of Section 3 around 45° for β and around 60° for ψ, respectively in Figure 3.

According to the results in Figure 3, the first situation is completely associated with pure Love particle motion (Section 1 in Figures 2 and 3). There are dominating periods on the transverse component and the amplitudes on the other components are very small. The second situation is associated with pure Rayleigh particle motion (Section 2 in Figures 2 and 3). The ground motion on the horizontal plane is perfectly radial and the amplitude on the tangential component is rapidly decreasing. In both cases, it is shown that the weighted functions of FFP are perfectly compatible with the angular distribution of polarization parameters in Figure 3. This means that FFP is able to weight Love wave amplitudes in Section 1 of Figure 2 and Rayleigh wave amplitudes in Section 2 of Figure 2.

In contrast, the weighted functions of FFP are not very compatible with the angular distribution of polarization parameters around 45° (for β) and around 70° (for ψ) in Section 3 of Figure 3. This means that the weighted functions of FFP are not exactly able to weight the fundamental mode surface wave amplitudes around 45° (for β) and around 70° (for ψ) because of interactions between particle motions. In addition, for the full length Love wave (Sections 1 and 3 in Figure 3) and for the full length Rayleigh wave (Sections 2 and 3 in Figure 3), the weighted functions of FFP are not compatible with the angular distribution of polarization parameters around 45° (for β) and around 70° (for ψ). For this reason, fundamental mode Love wave and initial parts of fundamental mode Rayleigh waves are deformed after FFP processing.

Hence, the weighted functions of FFP need be rearranged for better performance around 45° (for β) and around 70° (for ψ). In the proposed filtering process (NFP), the weighted functions used in

Table 1. The first set of parameters used in computing synthetic seismograms.

Crustal model						
Layer number	Thickness (km)	P-velocity (km s^{-1})	S-velocity (km s^{-1})	Density (g/cm^3)	Quality factors	
					Q_α	Q_β
1	1.50	4.30	2.60	2.10	300	150
2	3.00	5.25	3.15	2.40	250	125
3	4.50	5.80	3.60	2.60	200	100
4	7.50	6.20	3.90	2.80	150	75
5	15.0	6.70	4.20	3.00	100	50
6	∞	8.10	4.70	3.40	50	25

Table 2. The second set of parameters used in computing synthetic seismograms.

Source parameters	
Rake	180°
Dip	90°
Strike	90°
Azimuth	180°
Focal depth	10 km
Epicentral distance	1200 km

FFP are made perfectly compatible with the angular distribution of polarization parameters. Also, the weighted functions of NFP are able to strengthen the fundamental mode surface wave amplitudes. FFP is modified by the following new equations:

$$A_Z^{'}(\eta f) = A_Z(\eta f).WF_1^{M_1}[\beta(\eta f)].\cos^K[\psi(\eta f)-\theta].\sin^N[\alpha(\eta f)] \quad (4a)$$

$$A_R^{'}(\eta f) = A_R(\eta f).WF_1^{M_1}[\beta(\eta f)].\cos^K[\psi(\eta f)-\theta].\sin^N[\alpha(\eta f)] \quad (4b)$$

$$A_T^{'}(\eta f) = A_T(\eta f).WF_2^{M_2}[\beta(\eta f)].\sin^K[\psi(\eta f)+\theta/2] \quad (4c)$$

Herein

$$WF_1[\beta(\eta f)] = \begin{cases} 0.95+\left(+0.05.\cos^4\left(2.\beta(\eta f)\right)\right) & \beta(\eta f) \le \pi/4 \\ 0.95+\left(-0.95.\cos^4\left(2.\beta(\eta f)\right)\right) & \beta(\eta f) > \pi/4 \end{cases}$$

$$WF_2[\beta(\eta f)] = \begin{cases} 0.95+\left(-0.95.\cos^4\left(2.\beta(\eta f)\right)\right) & \beta(\eta f) \le \pi/4 \\ 0.95+\left(+0.05.\cos^4\left(2.\beta(\eta f)\right)\right) & \beta(\eta f) > \pi/4 \end{cases}$$

The weighted functions of NFP (WF_1 [β(ηf)] and WF_2 [β(ηf)]) were entirely derived from orthogonal functions of sine and cosine by trial and error to be compatible with the angular distribution of synthetic polarization parameters in Figure 4. The coefficients M_1 = 14 and M_2 = 14 are determined empirically. Also, the weighted function sin[(ψ(ηf)] in FFP is modified as sin[(ψ(ηf)+θ/2)] to be compatible with the polarization parameters. In a similar way, the coefficient K = 8 and horizontal/vertical displacement ratio θ/2 = 18.9 for the function sin[(ψ(ηf)+θ/2)] are determined empirically. The weighted functions sin[α(ηf)] and cos[ψ(ηf)-θ] in FFP are kept in NFP. The weighted functions of FFP and NFP are given in Figure 5.

COMPARISON OF FORMER AND NEW FILTERING PROCESSES

The filtering process is performed in several steps. All amplitudes in each component are normalized. For a selected WL and MI, Fast Fourier transforms of seismograms are calculated. In frequency domain, amplitude coefficients in each frequency are weighted. The weighted amplitudes are then transformed back to time domain. From arithmetical averages of overlapping amplitudes, filtered signal is obtained. To alleviate the windowing effect, Butterworth low-pass filtering and rounding are applied.

In this study, 10% cos tapering is applied to the edges of the WL. Addition of the lengths of 10% cos tapering to the maximum period (MP) of the seismogram gives the WL. Depending on WL, MI is determined after trial and error. This procedure can be formulated as follows:

WL - 2(10% cos tapering of WL) = MP

WL - 0.2WL = MP

WL = MP/0.8 (5a)

Ratio = WL/MI

MI = WL/Ratio (5b)

The ratio of WL/MI was given by Simons (1968) as 16. But, synthetic tests for all ranges of epicentral distances show that ratio 1.25 fits better than 16 to provide satisfactory time-frequency resolution and do not deform wave forms as shown in Figure 6.

The synthetic seismograms in Figure 2 were again utilized in Figure 7 to test FFP against NFP. Both filtering processes are not good at weighting the high frequency content of the wave forms due to the effect of windowing, low-pass filtering and rounding errors. FFP appears to fail on the initial part of the fundamental mode Rayleigh wave and on the main part of the fundamental mode Love wave. In general, NFP is better than FFP to recover the fundamental mode signals.

Table 3. Focal parameters of events used in this study.

S/N	Date (mo/d/yr)	Time (h:min:s)	Latitude (N°)	Longitude (E°)	Depth (km)	Magnitude (Ms)
1	12/26/2003	01:56:56	29.01	58.27	33.0	6.7
2	01/23/2005	22:36:08	35.95	29.71	31.9	5.4

Soruce: Incorporated Research Institutions For Seismology (IRIS).

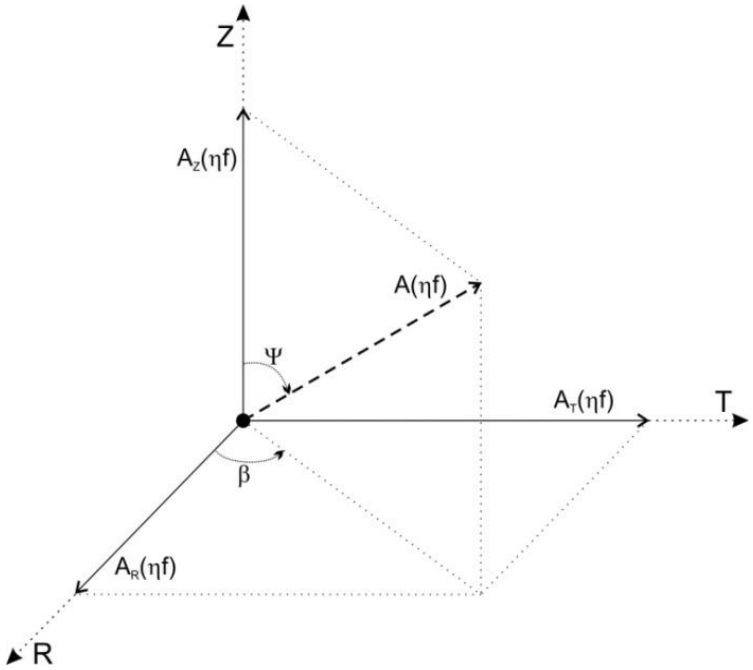

Figure 1. Components of the ground motion.

Both filtering processes were also applied on two three-component broadband digital seismograms recorded at TBZ station of Karadeniz Technical University, Department of Geophysics, Trabzon, Turkey given in Table 3.

The original traces (unfiltered), filtered traces (using FFP) and filtered traces (using NFP) for Event 1 in Table 3 with an epicentral distance of 2137 km are shown in Figure 8. Both filtering processes are successful to weight all parts of the fundamental mode Rayleigh waves in each component (from arrow 1 to the end). NFP has a noticeable achievement here (from arrow 2 to the end), whereas FFP fails in the initial part of the fundamental mode Love wave (Arrow 3).

The original traces (unfiltered), filtered traces (using FFP) and filtered traces (using NFP) for Event 2 in Table 3 with an epicentral distance of 1178 km are shown in Figure 9. NFP is more successful than FFP in terms of weighting the initial part of the fundamental mode Love and Rayleigh waves in each component (from arrow 1 to the end for Rayleigh waves, arrow 3 for Love wave). Herein, it is clear that when the epicentral distance gets smaller, FFP fails on the initial part of Love and Rayleigh waves in each component. NFP is able to weight all parts of fundamental Love and Rayleigh waves to achieve significant improvement over FFP (Figures 7, 8, and 9).

DISCUSSION

All amplitudes are normalized to avoid complications from amplitude interactions between components. When normalization is not employed, both processes may result abnormal amplitudes because both FFP and NFP are extremely sensitive to amplitude ratios between components. On the other hand, normalization may adversely affect the result of the filtering process. To avoid amplitude interactions between components, relatively high quality data sets should be utilized. In this study, a fixed WL and MI are used for the whole traces. Because surface waves are dispersive, changing WL and MI can be devised instead of fixing them.

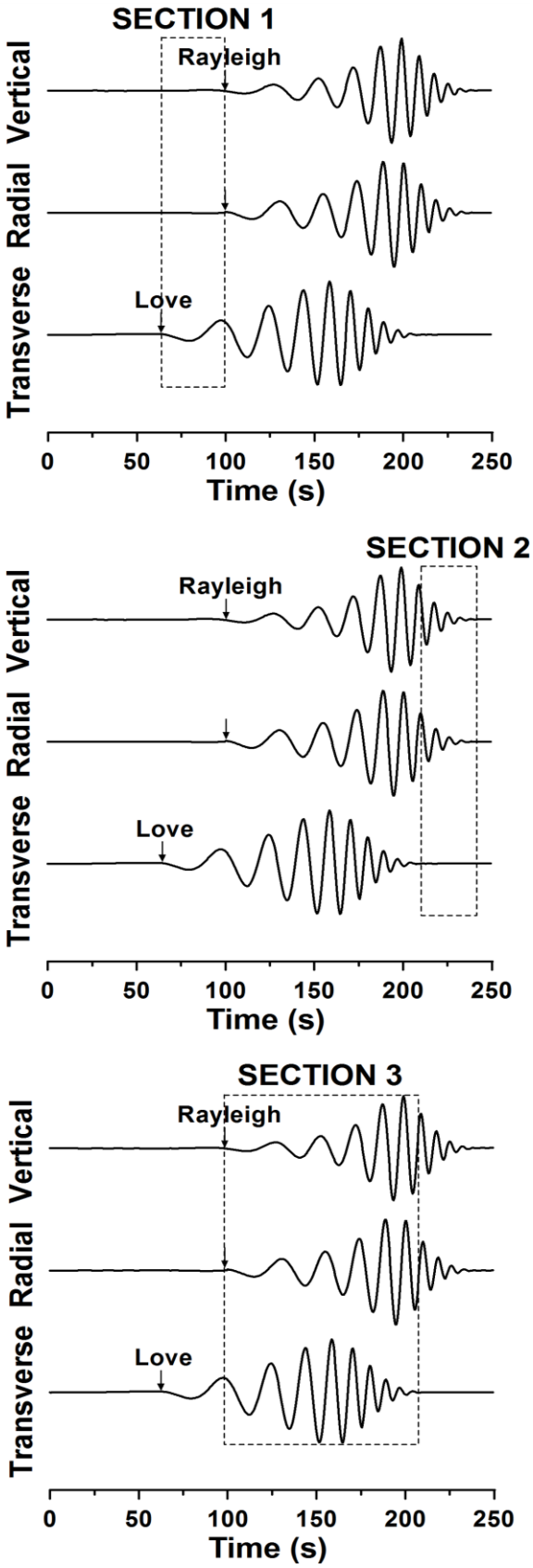

Figure 2. Time sections used to analyze synthetic polarization parameters.

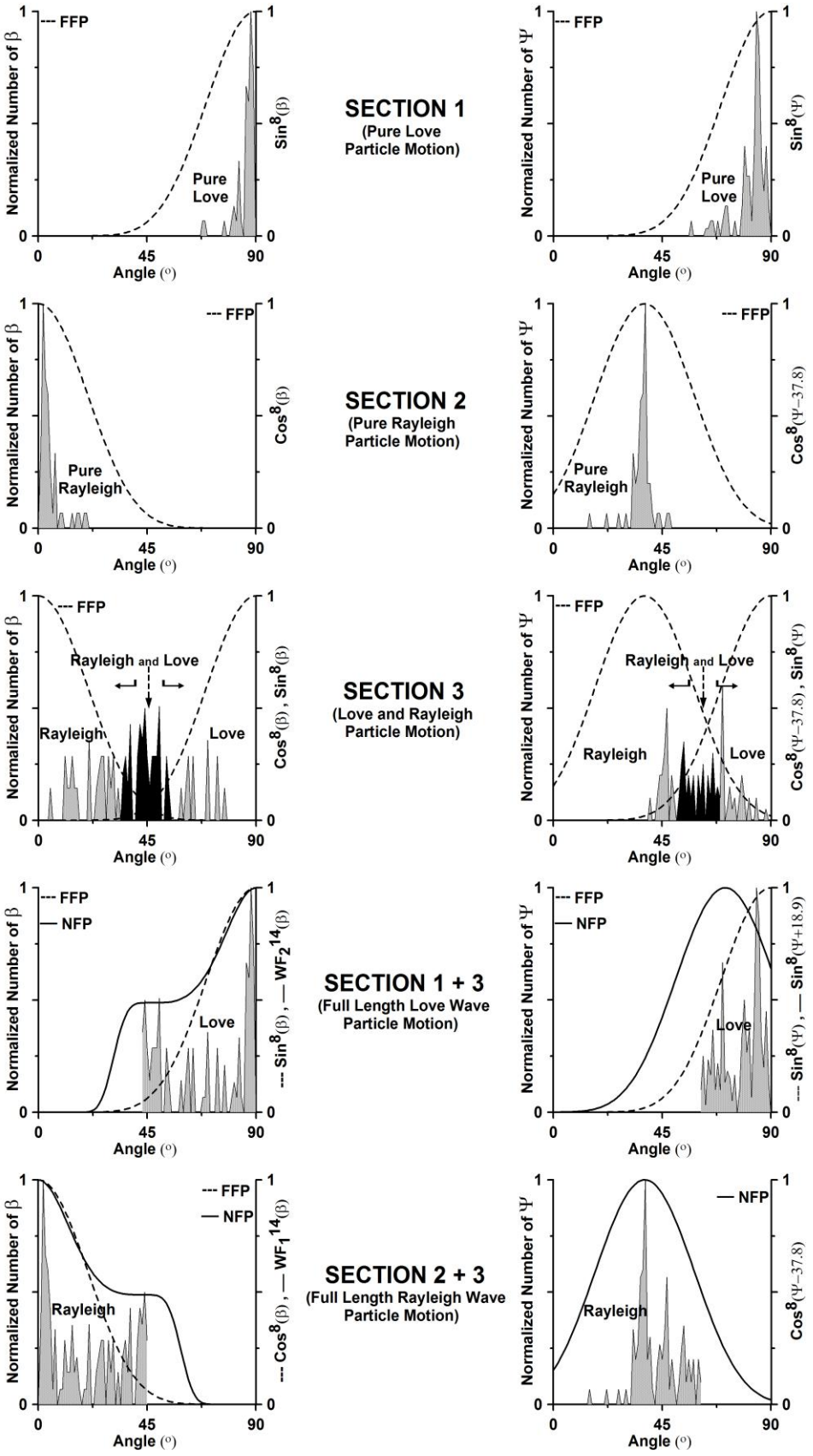

Figure 3. Investigation of compatibility between angular distribution of polarization properties and weighted functions of FFP and NFP in each section.

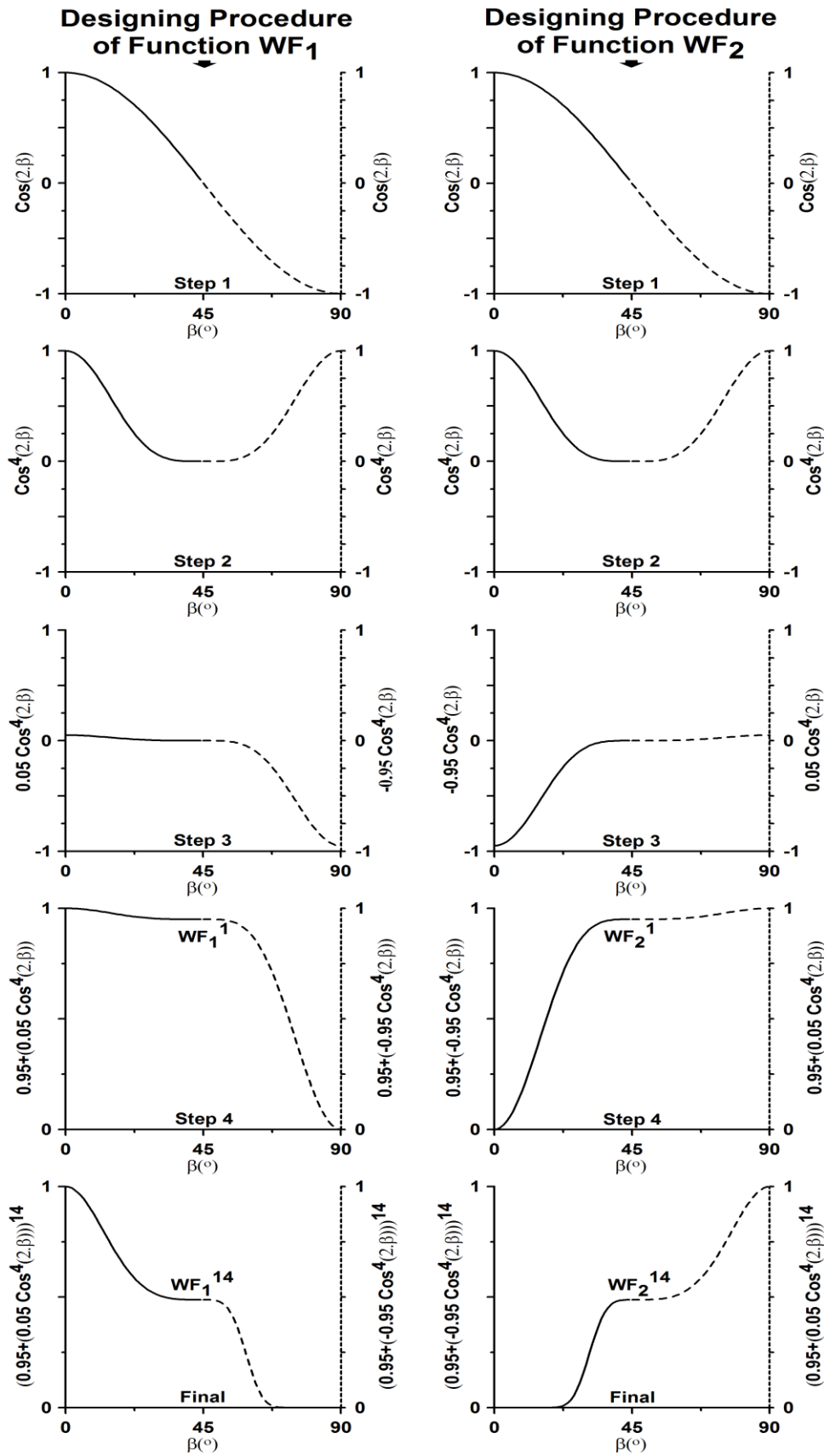

Figure 4. Designing procedures of functions WF_1 and WF_2 step by step.

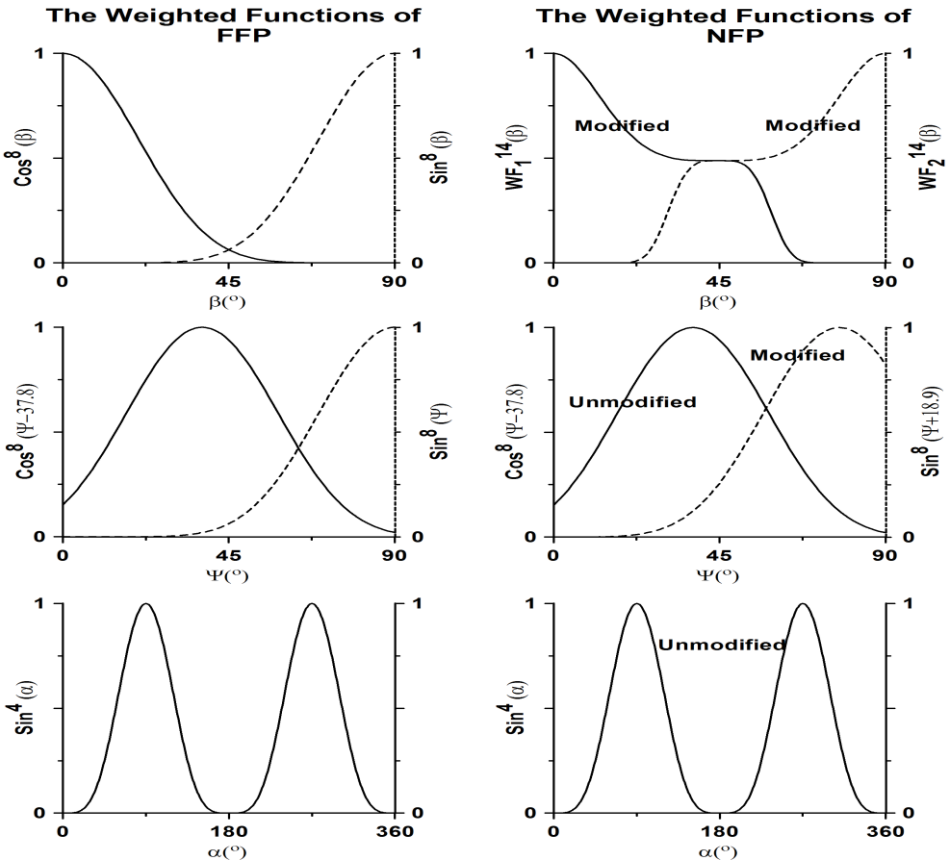

Figure 5. Weighted functions of FFP and NFP.

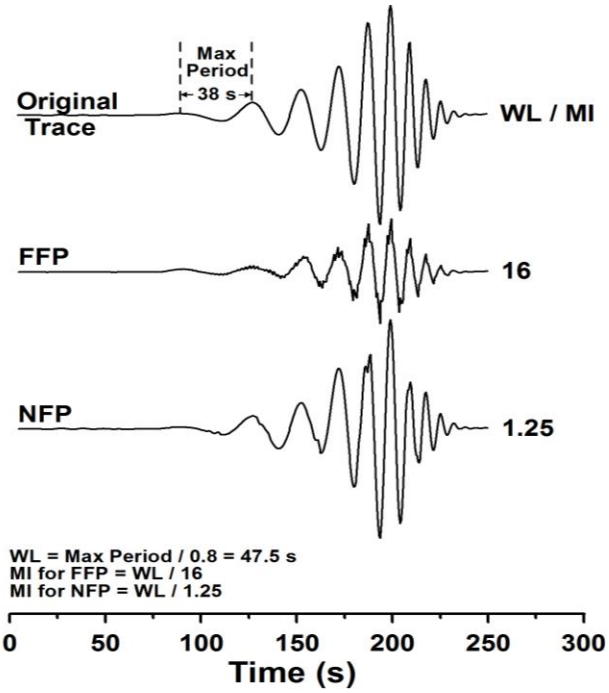

Figure 6. The effect of windowing process on seismograms.

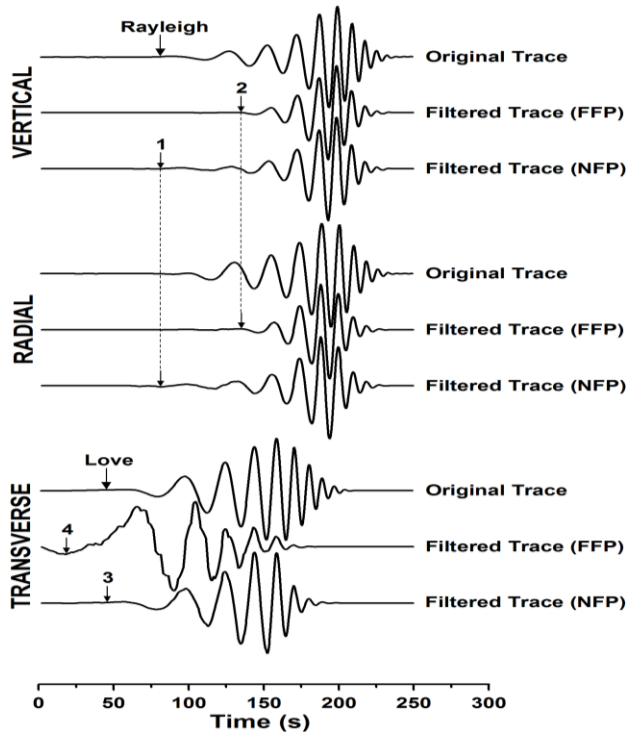

Figure 7. Original and filtered traces of synthetic seismograms.

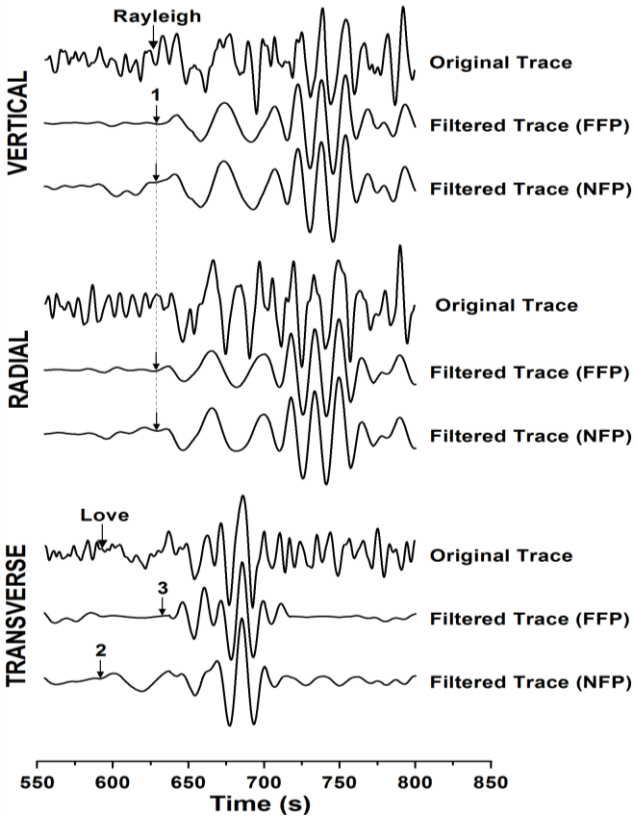

Figure 8. Original and filtered traces of Event 1 in Table 3.

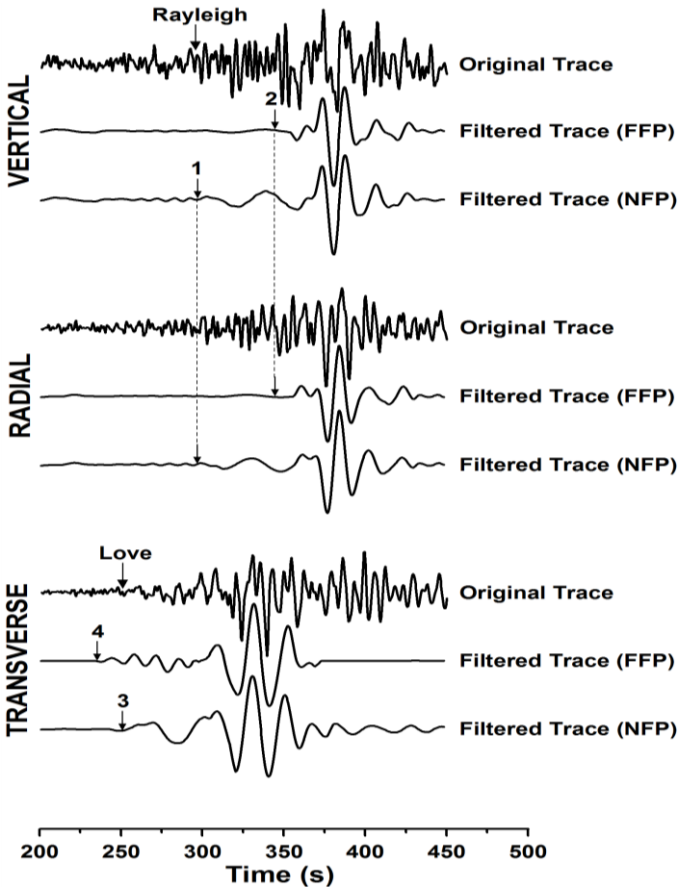

Figure 9. Filtered and unfiltered traces of Event 2 in Table 3.

FFP was modified to provide a better fit for the angular distribution of the synthetic polarization parameters derived from different time intervals. NFP given in Equations 4a, b and c is good for all epicentral distance ranges including epicentral distances smaller than ~20°. As a result, NFP is found better than FFP about weighting the fundamental mode Love and Rayleigh waves, and NFP can be safely used at all ranges of epicentral distances.

ACKNOWLEDGEMENT

We are very grateful to the Department of Geophysics, Karadeniz Technical University for the two broadband digital records used in this study.

REFERENCES

Amoroso O, Maercklin N, Zollo A (2012). S-wave identification by polarization filtering and waveform coherence analyses. Bull. Seism. Soc. Am. 102(2):854-861.

Blandford RR (1977). Discrimination between earthquakes and underground explosions. Ann. Rev. Earth. Planet. Sci. 5:111-122.

Blandford RR (1982). Seismic event discrimination. Bull. Seism. Soc. Am. 72(6):69-87.

Chael EP (1997). An automated Rayleigh-wave detection algorithm. Bull. Seism. Soc. Am. 87(1):157-163.

De Meersman K, van der Baan A, Kendall JM (2006). Signal extraction and automated polarization analysis of multicomponent array data. Bull. Seism. Soc. Am. 96(6):2415-2430.

Du Z, Foulger GR, Weijian M (2000). Noise reduction for broad-band three-component seismograms using data-adaptive polarization filters. Geophys. J. Int. 141:820-828.

Flinn EA (1965). Signal analysis using rectilinearity and direction of particle motion. Proc. IEEE. 53:1874-1876.

Holcomb LG (1980). Microseisms: A twenty-six-second spectral line in long-period earth motion. Bull. Seism. Soc. Am. 70(4):1055-1070.

Jurkevics A (1988). Polarization analysis of 3-component array data. Bull. Seism. Soc. Am. 78(5):1725-1743.

Kanasewich ER (1981). Time sequence analysis in geophysics, The University of Alberta Press, Edmonton.

Lilly JM, Park J (1995). Multiwavelet spectral and polarization analysis of seismic records. Geophys. J. Int. 122:1001-1021.

Montalbetti JF, Kanasewich ER (1970). Enhancement of teleseismic body phases with a polarization filter. Geophys. J. R. Astr. Soc. 21:119-129.

Morozov IB, Smithson SB (1996). Instantaneous polarization attributes and directional filtering. Geophysics 61:872-881.

Patane D, Ferrari F (1997). Seismpol_A visual-basic computer program for interactive and automatic earthquake waveform analysis. Comput. Geosci. 23(9):1005-1012.

Perelberg AI, Hornbostel SC (1994). Applications of seismic polarization analysis. Geophysics 59:119-130.

Pinnegar CR (2006). Polarization analysis and polarization filtering of three-component signals with the time-frequency S transform. Geophys. J. Int. 165(2):596-606.
Plesinger A, Hellweg M, Seidl D (1986). Interactive high-resolution polarization analysis of broad-band seismograms. 59:129-139.
Samson JC (1977). Matrix and Stokes vector representations of detectors for polarized waveforms: theory, with some applications to teleseismic waves. Geophys. J. Int. 51(3):583-603.
Samson JC, Olson JV (1980). Some comments on the descriptions of the polarization states of waves. Geophys. J. R. Astr. Soc. 61:115-129.
Selby ND (2001). Association of Rayleigh waves using backazimuth measurements: Application to test ban verification. Bull. Seism. Soc. Am. 91(3):580-593.
Shieh CF, Herrmann RB (1990). Ground roll: Rejection using polarization filters. Geophysics 55(9):1216-1222.
Shimsoni M, Smith SW (1964). Seismic signal enhancement three-component detectors. Geophysics 24:664-671.
Simons RS (1968). A surface wave particle motion discrimination process. Bull. Seism. Soc. Am. 58:629-637.
Vidale JE (1986). Complex polarization analysis of particle motion. Bull. seism. Soc. Am. 76(5):1393-1405.